



# Wear simulation of worm gears based on an energetic approach

K. Daubach<sup>1</sup> · M. Oehler<sup>1</sup> · B. Sauer<sup>1</sup>

Received: 26 March 2021 / Accepted: 19 July 2021 / Published online: 15 September 2021  
© The Author(s) 2021

## Abstract

Wear phenomena in worm gears are dependent on the size of the gears. Whereas larger gears are mainly affected by fatigue wear, abrasive wear is predominant in smaller gears. In this context a simulation model for abrasive wear of worm gears was developed, which is based on an energetic wear equation. This approach associates wear with solid friction energy occurring in the tooth contact. The physically-based wear simulation model includes a tooth contact analysis and tribological calculation to determine the local solid tooth friction and wear. The calculation is iterated with the modified tooth flank geometry of the worm wheel, in order to consider the influence of wear on the tooth contact. Experimental results on worm gears are used to determine the wear model parameter and to validate the model. A simulative study for a wide range of worm gear geometries was conducted to investigate the influence of geometry and operating conditions on abrasive wear.

## Verschleißsimulation von Schneckengetrieben mit energetischem Berechnungsansatz

### Zusammenfassung

Abhängig von der Baugröße des Schneckengetriebes treten unterschiedliche Verschleißformen an der Schneckenverzahnung vorwiegend auf. In großen Getrieben ist dies häufig Ermüdungverschleiß in Form von Grübchen, wohingegen bei kleineren Getrieben meist abrasiver Verschleiß vorherrschend ist. Im Rahmen einer Untersuchung zum abrasiven Verschleiß von Schneckengetrieben wurde ein Simulationsmodell entwickelt, mit welchem Verschleiß an Schneckenverzahnungen auf Basis eines energetischen Ansatzes vorhergesagt werden kann. Der lokale Verschleißberechnungsansatz verbindet Verschleiß mit der im Zahnkontakt entstehenden Festkörperreibungsenergie. Das physikalisch begründete Simulationsmodell beinhaltet eine Berechnung des Eingriffsfeldes und der tribologischen Größen im Zahnkontakt, um die Festkörperreibungsenergie und den Verschleiß lokal zu ermitteln. In der iterativen Verschleißsimulation erfolgt nach jedem Berechnungsschritt eine lokale Anpassung der Flankengeometrie des Schneckenradzahnes entsprechend der rechnerischen Verschleißabträge, um den Einfluss von Verschleiß auf den Zahnkontakt in den nachfolgenden Berechnungen zu berücksichtigen. Für die Ermittlung des Verschleißkoeffizienten des energetischen Modells sowie für die Validierung des Simulationsmodells wurden experimentelle Ergebnisse verwendet. Mit dem Simulationsmodell wurde weiterhin eine Parameterstudie durchgeführt, um Zusammenhänge zwischen geometrischen Verzahnungsgrößen, Betriebsbedingungen und Verschleiß zu untersuchen.

## 1 Introduction

Worm gears are used as transmission elements, where a high transmission ratio, a smooth operation and high load bear-

ing capacity is required. These characteristics are combined with a compact design of the gears in a single gear stage. The smooth operation is given by a relatively high contact ratio and the gear's kinematics, that include a substantial sliding motion of the worm relative to the contact point. In return, the sliding contact conditions are the reason for frictional power losses and in case of boundary friction also for wear. To prevent scuffing in tooth contact, the most common material combination is a bronze wheel and a hardened steel worm. The difference in hardness leads to wear mainly on the worm wheel.

---

✉ K. Daubach  
kevin.daubach@mv.uni-kl.de

<sup>1</sup> Institute of Machine Elements, Gear & Transmissions, Technische Universität Kaiserslautern, Gottlieb-Daimler-Str., 67663 Kaiserslautern, Germany

The main wear phenomena in worm gears with a bronze wheel and a steel worm are abrasive wear on the surface and fatigue wear in the subsurface. Abrasive wear occurs because of an insufficient lubricant film and sliding contact of surface asperities. The contact of two surfaces can be accompanied by wear particles in the lubricant which is termed as three body abrasive wear [1]. Fatigue wear appears in the form of pitting due to a too high stress level under cyclic pressure load. Here, a main factor for the load bearing capacity of worm gears is the size of the contact pattern. Usually, the worm wheel is manufactured with an oversized hob, resulting in a relatively small contact pattern in the first place. Furthermore, manufacturing errors as pitch errors are responsible for local stress concentration. At the beginning of the gear operation, abrasive wear on the worm wheel teeth increases the contact pattern and reduces thereby the contact pressure. This initial wear process (running-in) with severe wear rates is more pronounced in small than in large gear boxes, because of a lower entraining speed and thereby a poorer hydrodynamic lubricant film formation. Thus, large gears often do not reach a full contact pattern and load bearing capacity, leading to a higher risk for fatigue wear.

For the design of worm gears a precise estimation of wear for certain operating conditions is crucial. An efficient method for wear prediction is given by wear simulation models. The main objective of the herein presented wear model and the simulative wear study is abrasive wear. The energetic wear model of Fleischer [2] is used to calculate wear based on friction energy transferred into the tribological contact. The wear model is coupled with a physical-based simulation model for friction in worm gears.

## 2 State of the art

In literature, several studies on wear modelling and calculation can be found. A detailed overview of the different approaches is given in [3]. In most cases wear is calculated based on the contact pressure using the empirical model of Archard [4]. The model includes furthermore the hardness of the softer material in contact, the sliding distance and an experimentally determined wear coefficient. Jbily et al. implemented this model in their numerical wear calculation of worm gears [5]. The wear coefficient was defined locally for each contact point by the ratio of local lubricant film thickness and surface roughness. Sharif et al. modified the model of Archard to calculate local wear in worm gears [6]. The original model was supplemented with the sliding speed and a modified ratio of local lubricant film thickness and surface roughness.

Pausch [7] developed a wear model based on the assumption, that wear is a result of the penetration of roughness

asperities of both contact surfaces. His model includes a statistical description of the surface roughness. Wear is locally applied when the calculated film thickness is smaller than a local surface roughness parameter.

## 3 Wear modelling based on frictional energy

Under realistic operating conditions, the lubricated contact of the tooth flanks of worm gears can be assigned to the mixed friction regime. This means that the asperities of the surfaces are in contact with each other at certain points (boundary friction), but at other points these asperities are separated from each other by a lubricant film (fluid friction). Depending on the local tribological conditions, boundary or fluid friction predominates at one point.

Boundary friction is a result of elastic and plastic deformation of asperities of the two surfaces in contact [1]. For a relative movement of the tooth flank surfaces in worm gears, frictional energy is required to sustain sliding. Cutting by harder asperities of the worm surface or repeated plastic deformations along the sliding distance of multiple tooth contacts finally lead to wear on the worm wheel. Depending on the tribological conditions, different wear mechanisms are superimposed. However, the physical basis is considered to be frictional energy. By using an energetic approach for wear calculation, especially in combination with a physically-based simulation model for friction, valid results for various gear geometries as well as tribological conditions are expected.

Fleischer introduced an approach to describe wear in tribological contacts based on friction energy [2], which also includes a concept for cumulative damage. With relative motion of both contacting surfaces (sliding) friction energy is transferred, which is for the most part dissipated as heat energy. A part of the friction energy is stored in the material as lattice defects caused by mechanical deformations. When the accumulated energy reaches a critical level in a local volume of material, material fractures and wear particles form. The critical energy level is given by the wear energy density  $e_R^*$ , which represents the central parameter of the wear model of Fleischer and quantifies the linear relationship between frictional energy  $W_R$  and the volumetric wear removal  $V_v$  (Eq. 1).

$$V_v = \frac{W_R}{e_R^*} \quad (1)$$

From this equation can be concluded that a higher wear energy density results in a higher wear resistance and to less wear. According to [2] the wear energy density can be calculated based on theoretical considerations. However, in related literature values were often determined with experimental data [8–10].

### 3.1 Tribological simulation of worm gears

The simulation of tribological conditions in the tooth contact of worm gears has been subject of research at MEGT for some time. In this context, a simulation tool was developed with which the coefficient of friction in the tooth contact of worm gears can be reliably determined [11]. The simulation tool is based on the work of Predki [12] and Bouché [13]. The individual components of the simulation are, on the one hand, an analysis of the geometry and kinematics of the gears in order to be able to map contact lines, local velocity and radii of curvature. Furthermore, a locally resolved lubricating gap height calculation is carried out with approximating equations for the elasto-hydrodynamic contact. In addition, a relationship between the lubricating gap height and the solid body contact ratio is derived with the help of an outsourced contact simulation based on the half-space theory [11]. This parameter describes the proportion of the contact pressure that is applied directly to the contacting metallic surfaces. It is used to determine the local division of friction into boundary and fluid friction. The relationship of gap height and solid body contact ratio can be described by an approximation equation and thus integrated into the tribological simulation in a computationally efficient manner. For this purpose, real measured three-dimensional surfaces of the tooth flanks of worm and worm wheel are used as input files. In this way, a local solid body contact ratio can be determined for each discretization point of the calculation area. With the help of this parameter, boundary friction and fluid friction are then weighted and combined into a mean coefficient of friction in the mixed friction regime. The boundary friction coefficient is determined by twin disc tribometer tests. The internal friction of the lubricant is determined with the model according to Bair and Winer under the assumption of a pseudoplastic fluid behaviour. Data on the lubricant used are obtained from measurements in a high-pressure viscometer.

The total friction in the tooth contact can finally be determined by integrating the local mixed friction coefficient over the entire contact area of every specific meshing position. Together with the losses of the bearings and seals as well as the hydraulic losses in the gearbox, the overall efficiency of worm gearboxes can thus be calculated. The workflow of the tribological simulation is described more detailed in [14].

For a local wear calculation, the friction components due to solid body contact as well as the contact pressure, which must be absorbed directly by the surface asperities, are particularly relevant. These parameters are described here with the help of the boundary friction coefficient, the flank pressure and the solid body contact ratio at each discretization point of the meshing area. The meshing area is discretized

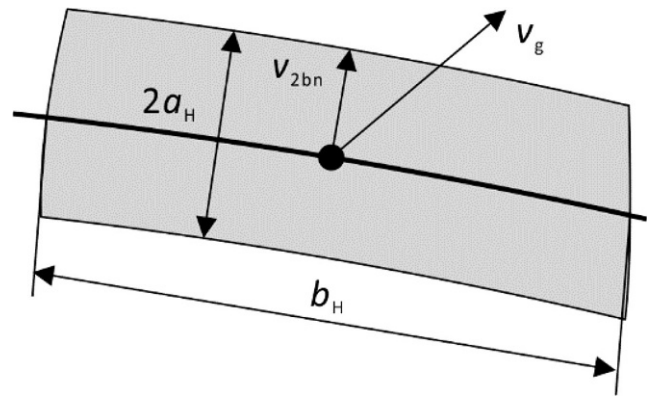


**Fig. 1** Contact line segment with the dimensions of the Hertz'ian contact area  $a_H$  and  $b_H$ , the sliding velocity  $v_g$  and the velocity  $v_{2bn}$

in contact lines of a specified number of mesh positions and contact points that divide each contact line in segments.

### 3.2 Local wear calculation

With the tribological simulation, friction can be calculated locally for each contact point of the discretised tooth contact. Local friction work  $W_R$ , required as input for the energetic wear model to calculate the volume loss  $V_v$ , is a result of friction force  $F_R$  and sliding distance  $s_R$  and yields with Eq. 1 in:

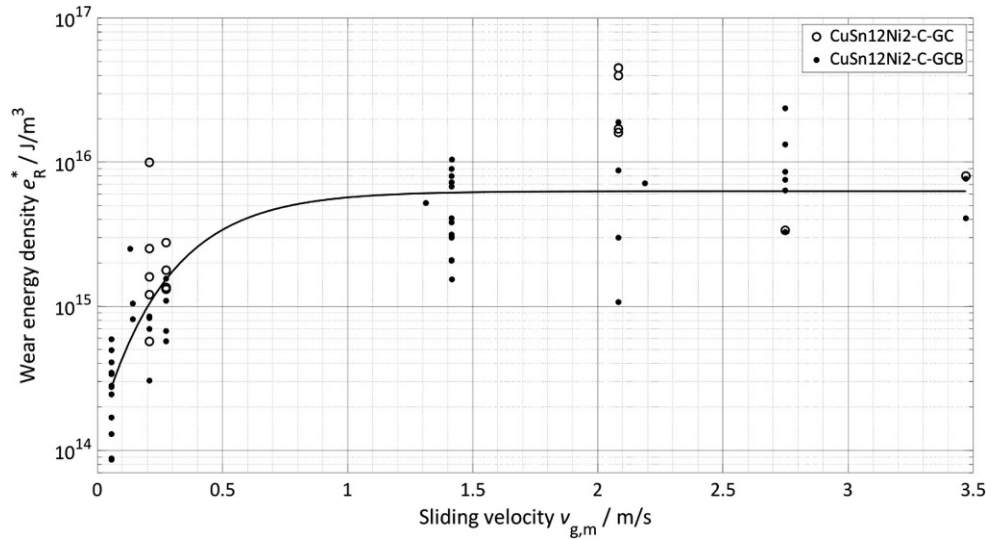
$$V_v = \frac{1}{e_{R^*}} \cdot W_R = \frac{1}{e_{R^*}} \cdot F_R \cdot s_R \quad (2)$$

Load is described in the tribological simulation with a local line load  $w_b$  applied on each contact line segment with an individual length  $b_H$ . The tooth contact of each line segment is modelled as a Hertz'ian contact between two cylinders, leading to a contact surface with the length of the segment  $b_H$  and twice the half width  $a_H$  (see Fig. 1). Since the solid body friction is relevant for abrasive wear, only the proportion of the load related to the solid body contact ratio  $\psi$  is considered. Together with the local boundary friction coefficient  $\mu_{Gr}$  the wear relevant friction force  $F_R$  is given by Eq. 3.

$$F_R = w_b \cdot b_H \cdot \mu_{Gr} \cdot \psi \quad (3)$$

During gear operation each contact point is transferring load for a certain time  $t_c$ . In tooth contact, sliding of both surfaces occurs due to the gear kinematics, quantified by the sliding velocity  $v_g$ . The contact time  $t_c$  depends on the half width  $a_H$  and the velocity  $v_{2bn}$  of the contact point when passing over the contact area. The velocity  $v_{2bn}$  is the sliding speed component in normal direction to the contact line

**Fig. 2** Results for the wear energy density  $e_R^*$  with respect to the respective mean sliding velocity  $v_{g,m}$



[12]. The sliding distance  $s_R$  each contact point experiences during contact is then calculated according to Eq. 4.

$$s_R = v_g \cdot t_c = v_g \cdot \frac{2a_H}{v_{2bn}} \tag{4}$$

The local wear volume is simplified as a cuboid volume with the Hertzian contact area  $A = 2a_H \cdot b_H$  as base area. The height is then equal to the local wear height  $\delta_v$  and calculated using Eq. 5. With the simplification that wear only occurs on the worm wheel, the macro geometry of the worm wheel tooth is for each point individually modified by a tangential displacement with the respective calculated wear height. The modification is applied on all wheel teeth in equal measure.

$$\delta_v = \frac{1}{e_R^*} \cdot w_b \cdot \mu_{Gr} \cdot \psi \cdot \frac{v_g}{v_{2bn}} \tag{5}$$

The micro geometry of the worm wheel surface is unaffected by this modification. However, the microstructure of the surface changes during wear process. To consider this effect in the tribological calculations, real measured three-dimensional surfaces are also acquired for worn surfaces and evaluated with the contact simulation in terms of solid body contact ratio (see Sect. 3.1).

### 3.3 Determination of the wear model parameter $e_R^*$

To adjust the energetic wear model on the tooth contact of worm gears the wear energy density was determined experimentally. Due to their kinematics and geometry, worm gears represent a complex tribological system with large local differences regarding the contact conditions. For that reason, measurement data was taken from wear tests on the original tribological system. The tests were performed

with worm gears with a centre distance of 32 mm, 40 mm and 50 mm under various load and speed conditions. Within a single test, output torque and input speed were constant over the entire time period. As lubrication, polyglycol-based oil with a viscosity class ISO VG 220 was used. The worm wheels were made from continuous cast bronze CuSn12Ni-C-GC (UNS C91700) and the worms from steel 16MnCr5 (1.7131/AISI 5110). All gears were preconditioned and had a full contact pattern before the wear tests, by which a steady wear rate could be expected from the very beginning. The simulative study presented in this article (see Sect. 5.3) was focused on worm gears that are operating in the steady wear phase, which requires values for the wear energy density related to this phase.

Wear was determined by measuring the mass loss of the worm wheel and converted into a volume loss with the density of the bronze material  $\rho = 8.8 \text{ g/cm}^3$ . The volume loss was equally distributed on all teeth of the worm wheel and load cycles for each tooth.

The related friction work  $W_R$  for a single tooth and complete mesh period was computed with the numerical tribological simulation program. Since friction in worm gear tooth contact varies during the gear meshing, friction power loss  $P_R$  needs to be integrated over time to obtain friction work. In the case of discretized meshing, friction power loss  $P_{R,i}$  was evaluated for all discrete mesh positions and multiplied with time  $\Delta t$  between two mesh positions.

$$W_R = \int P_R dt \approx \sum_i P_{R,i} \cdot \Delta t \tag{6}$$

The wear energy density  $e_R^*$  is then given by the ratio of friction work and volume loss according to Eq. 1. The obtained wear energy densities of in total 66 wear tests show

a large scattering, which is partly due to a dependency of the mean sliding velocity in tooth contact (see Fig. 2). The results indicate an increasing wear energy density with an increasing sliding velocity. The diagram includes values of the standard cast bronze (CuSn12Ni-C-GC) and the treated cast bronze (CuSn12Ni-C-GCB). Both materials are relevant for industrial worm wheel manufacturing. A similar dependency between both parameters was found for a material combination brass/steel in [9]. Here, the wear energy density seems to approach a constant value for higher sliding velocities. For illustration of this characteristic, an exponential function was used to fit the mean values at each sliding velocity level.

One reason for the remaining scattering at test points with the same sliding velocity is variation of up to a factor of three in the measured wear, even under the same test conditions and nominally identical gears. In contrary, such differences cannot be represented within the calculation of the friction work, which results in a variation of the wear energy density for the respective test point.

In addition, the mean flank pressure differs among all test points with the same sliding speed due to different load conditions, which could also contribute to the scattering here. According to the results in [8, 9], the wear energy density is influenced by the mean contact pressure. However, based on the available data, no clear pressure dependence of the wear energy density could be found.

#### 4 Procedure of wear simulation

The presented wear model was included in a worm gear simulation cluster of the tribological simulation and the external software for worm gear design *SNETRA*, which is used to calculate the local flank pressure as well as the initial discretised worm wheel geometry for the wear simulation. A detailed explanation on the computation in *SNETRA* is given in [15]. The wear simulation is designed as an iterative procedure, initiated with a wear calculation with

the initial, manufactured gear geometry. In all subsequent calculation steps the wear-modified geometry of the wheel tooth is used to consider the effect on wear on the tribological calculations.

The change of the macro geometry of worm wheel has an effect on the flank pressure distribution within a single mesh position. During running-in the length of the contact lines increases, which reduces the mean flank pressure. In addition, the local wear calculation based on an energetic model leads to higher wear for contact points that are more subjected to boundary friction. As a result, the pressure load moves gradually from points with a higher level of frictional energy to those with a lower level until the energy level is balanced. In the energetic equilibrium, the mean flank pressure is constant and wear occurs equally on all contact points, which is characteristic for the steady wear phase. These theoretical considerations are supported by results of wear on worm gears during running-in phase.

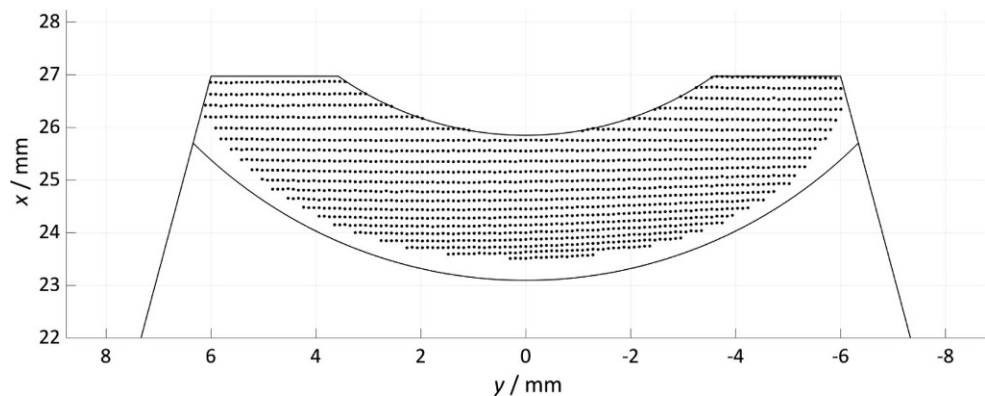
A single calculation step of the wear simulation consists of the following sequences:

1. Determination of contact lines and local velocities with a tooth contact analysis for the geometry of worm (initial) and worm wheel (initial/wear-modified)
2. Calculation of contact pressure distribution and transfer to the mesh of the tribological simulation
3. Determination of frictional energy and wear through local tribological analysis
4. Modification of the worm wheel according to the calculated wear

#### 5 Tooth contact analysis

The contact lines and local velocities of the worm gears are determined with an unloaded tooth contact analysis (TCA) in each calculation step. Here, a parameterised worm tooth flank according to [16] is paired with the discretised tooth flank of the worm wheel in the initial or a wear-modified condition. Load sharing is considered by including multiple

**Fig. 3** Contact lines of a worm gear obtained with the tooth contact analysis ( $a = 32$  mm,  $z_1 = 1$ ,  $z_2 = 39$ ,  $m_x = 1.25$  mm)



worm wheel teeth in the tooth contact analysis. The algorithm is based on equality of position vectors for worm and worm wheel, when located in a common coordinate system:

$$r_{2,i}(\Delta\varphi_2) = r_1(u, v, \varphi_1) \quad (7)$$

Where  $r_{2,i}$  represents the point with subscript  $i$  of the wheel tooth flank as a function of the wheel rotation angle  $\Delta\varphi_2$  and  $r_1$  the worm tooth flank geometry according to [16] as a function of the radius parameter  $u$ , the angle parameter  $v$  and the related mesh position angle  $\varphi_1$ .

The solution of Eq. 7 leads to the contact point on the worm flank as well as the required wheel rotation angle  $\Delta\varphi_2$  for a discrete mesh position for each relevant point of the worm wheel. A contact line is represented by points with a minimum wheel rotation angle. This procedure is repeated for multiple mesh position to determine all relevant points within the contact area for the current calculation stage (Fig. 3).

## 5.1 Concept of wear step and wear calibration

In a single load cycle of the gears a relatively small amount of wear emerges with only small changes of the tooth shape. It can therefore be assumed that over multiple load cycles the amount of absorbed friction energy and wear is approximately constant in a local tooth contact. In addition, the wear rate of worm gears decreases during the running-in phase, which leads to decreasing changes in the tooth shape between two calculation steps. To obtain an efficient computation, the concept of equal wear steps is introduced, where in every calculation step a comparable wear removal is applied. This includes furthermore, that the maximum value of the calculated wear height distribution of the entire contact area is compared to a specified wear step. The wear height distribution is then uniformly scaled according to the ratio of maximum wear height and wear step. The wear step is chosen as a balance between a continuous wear

process on the one hand and the computation time on the other hand.

Another difference to real gear meshing is the limited number of mesh positions evaluated in the wear simulation. Wear is only calculated for actual contact points with present flank pressure. For reasons of accuracy, wear is not interpolated on neighboured points within the contact area, that are theoretically involved in meshing and load transfer. This issue is shown schematically in Fig. 4 by contrasting discrete wear volumes obtained in the simulation and a continuous wear volume. For this reason, the calculated wear volume cannot be compared with the actual volumetric wear removal in a continuous meshing process.

In order to analyse wear with respect to time, wear calibration is required. A time-related value is given with the frictional energy that occurs per load cycle and tooth of the worm wheel. This value was also used for the determination of the wear energy density  $e_R^*$  (Eq. 6). With the energetic model (Eq. 1), a theoretical volumetric wear removal for a single tooth and load cycle is calculated based on the total frictional energy  $W_{R,i}$  of the current calculation step. The discrete, scaled volumetric wear removal  $V_{V,i}$  is calculated as a cuboid with the local wear height  $\delta_V$  and the local area given by the discretisation. A comparison of the discrete volumetric wear removal  $V_{V,i}$  with the theoretical volume according to Eq. 8 yields in the corresponding number of load cycles  $\Delta N_i$  for the current calculation step.

$$\Delta N_i = \frac{V_{V,i}}{\frac{W_{R,i}}{e_R^*}} \quad (8)$$

## 6 Results

### 6.1 Wear simulation of running-in

A wear simulation was carried out for a worm gear with a centre distance  $a=32$  mm and a gear ratio  $i=39$  with an incomplete initial contact pattern. Thus, an increase of the contact pattern could be expected within the simulation. The wear energy density was set to  $e_R^* = 2 \cdot 10^{13}$  J/m<sup>3</sup>. Contact patterns for four stages of the simulation are indicated in Fig. 5a–d with the area on the worm wheel flank affected by wear. The colourmap of the wear distribution after the first calculation step (see Fig. 5a) in particular illustrates the local differences of wear on the wheel flank, due to varying tribological conditions and flank pressure in tooth contact. Points of the wheel flank with the highest accumulated wear heights are located in the initial position of the contact pattern, since they are exposed to wear from the very first step. With the number of calculation steps, the accumulated wear on the wheel increases and the con-

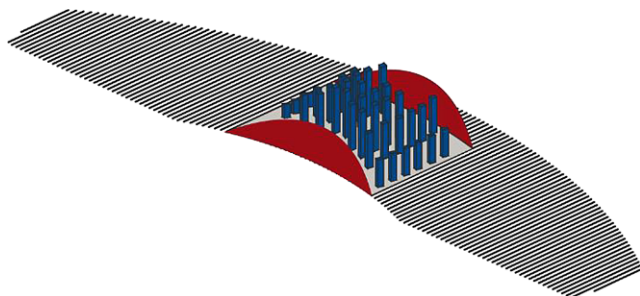


**Fig. 4** Discrete wear removal on the worm wheel (*blue cuboids*) in comparison with the theoretical continuous wear volume of a single load cycle indicated with red boundary surfaces

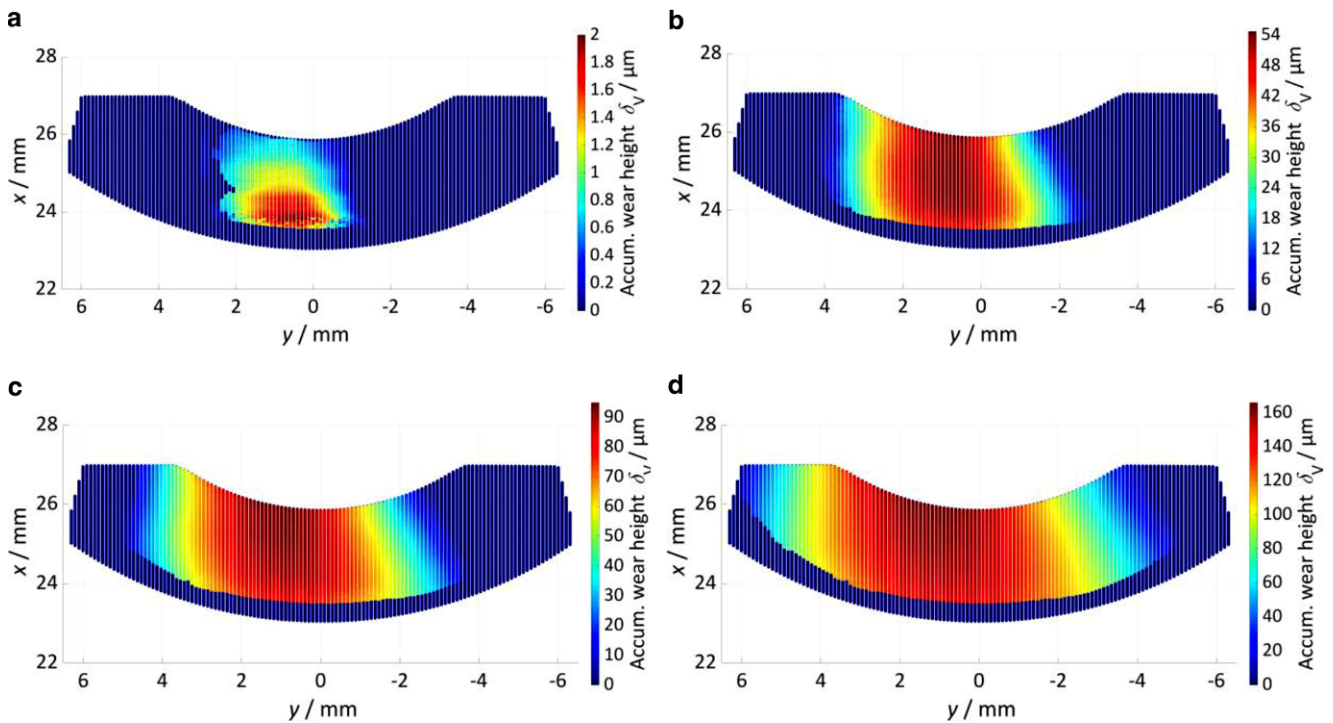
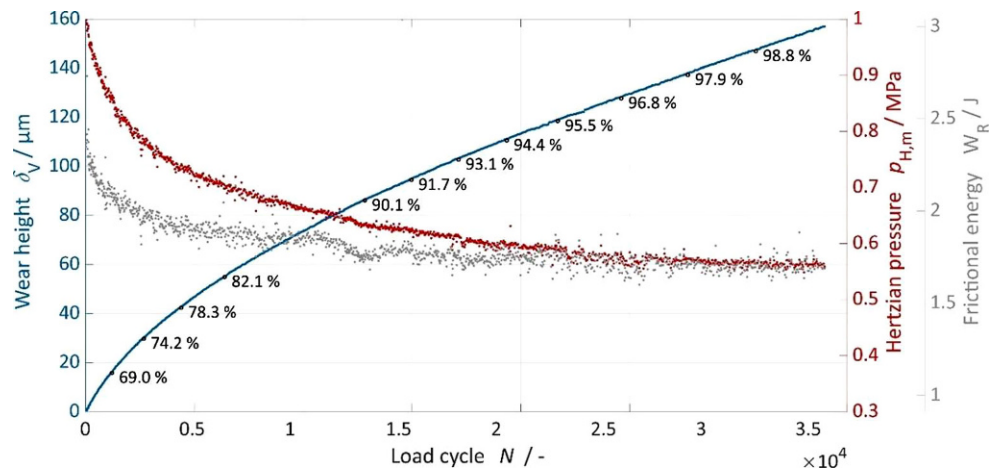


**Fig. 5** Accumulated wear height  $\delta_v$  on the worm wheel for the indicated calculation stages of the wear simulation for a worm gear during running-in phase ( $a=32\text{ mm}$ ,  $i=39$ ,  $n_1=150\text{ min}^{-1}$ ,  $T_2=32\text{ Nm}$ ). **a** After first step, **b** After 300 steps, **c** After 600 steps, **d** After 1200 steps

**Fig. 6** Calculated wear height, Hertzian pressure and total frictional energy per tooth and load cycle progression during running-in of a worm gear ( $a=32\text{ mm}$ ,  $i=39$ ,  $T_2=32\text{ Nm}$ ,  $n_1=150\text{ min}^{-1}$ ). The percentage proportion of the respective contact area related to the maximum contact area is additionally indicated



tact pattern expands. After 1200 stages (Fig. 5d) the contact pattern is almost completely developed.

Results for the maximum wear height mean flank pressure and total frictional energy (per wheel tooth and load cycle) progression with respect to load cycles are shown in Fig. 6. Furthermore, the percentage proportion of the respective contact area related to the maximum contact area is specified. The results indicate a typical behaviour for worm gears during running-in. The highest wear rate can be found at the beginning of the wear process. With an increasing wear height, the wear rate reduces and transitions into a linear progression, which is characteristic for the steady

wear phase. Complementary to the wear height progression, the initially high flank pressure decreases as a result of an expanding contact area and approaches asymptotically to a constant mean pressure level at the transition to the steady wear phase. Regarding the theoretical considerations of an energetic equilibrium in Sect. 4, the same progression as for the mean flank pressure can be found for the total frictional energy.

## 6.2 Comparison to experimental results

The wear simulation model was compared to experimental results of wear tests located in the running-in phase of worm gears. The test gears with a centre distance  $a=32$  mm and a gear ratio  $i=39$  had the same material and lubricant as those in the experiments of which the wear model parameter  $e_R^*$  was evaluated (see Sect. 3.3). This gives a good comparability in terms of results for the wear energy density, since the wear model is also adapted to wear measurements of the running-in wear tests with an individual wear energy density.

The initial contact pattern of the test gears was relatively small, as the wheels were manufactured with an oversized hob. The manufacturing parameters were set specifically for the generation of the wheel geometry in the simulation to achieve comparable initial contact patterns for experiment and simulation.

The wear tests were performed under constant operating conditions. The wear progress was monitored by regular measurement of the circumferential backlash for numerous mesh positions within one revolution of the worm wheel. The method described in [17] was applied to measure highly resolved backlash curves under low load contact conditions and to evaluate the backlash increase for identical mesh positions. According to [17], the backlash increase caused by wear varies within one pitch period, because of varying wear along the contact path and load sharing. The method includes moreover a concept of the transformation of the backlash increase to a wear height. In the wear tests, measured wear heights of all teeth were averaged to obtain representative values. For consistency reasons, the wear height was determined with the same method in the wear simula-

tion. In the simulation, the backlash increase was calculated within the tooth contact analysis (see Sect. 4.1).

The simulation of the running-in phase was conducted for different wear energy densities to find a good approximation of the wear model to the measured data points. Results for the wear height of the simulation model are compared to measured data of the experiments in Fig. 7. The data points of the experiments are supplemented by an interpolating curve. The curve refers to a fitted mathematical function, that was used in [18] to model the wear characteristics of chain drives.

The diagram shows three wear height progressions with different model parameters. In the first section of the experimental curve, the wear model with the lower wear energy density  $e_R^* = 1.5 \cdot 10^{13} \text{ J/m}^3$  provides a very good approximation. However, at some point the deviation to the experimental data increases significantly as a difference in wear rate. Assuming that the frictional energy is comparable in experiment and simulation, the lower wear rate in the experiment leads to the conclusion, that the wear energy density increases during the wear process. A reason could be the simultaneously decreasing mean flank pressure. Even if no clear dependence on pressure emerged from the analysis in Chapter Sect. 3.3, other related studies in [8, 9] show an increasing wear energy density in case of a decreasing pressure load, which is in good accordance with the observations from the comparison in Fig. 7.

When the simulation is carried out with the higher wear energy density  $e_R^* = 5.8 \cdot 10^{13} \text{ J/m}^3$ , the deviation to the experimental progression is high in terms of the absolute wear height. However, the wear rate at the end is approximately the same. As a consequence, a wear simulation was conducted with including a progressive characteristic of the wear energy density. The change of the model parameter

**Fig. 7** Comparison between simulative results with different model parameters  $e_R^*$  and wear measurement for a worm gear during running-in ( $a=32$  mm,  $i=39$ ,  $n_1=150 \text{ min}^{-1}$ ,  $T_2=32 \text{ Nm}$ ). The grey markers represent a computed wear progression with a gradually increasing model parameter

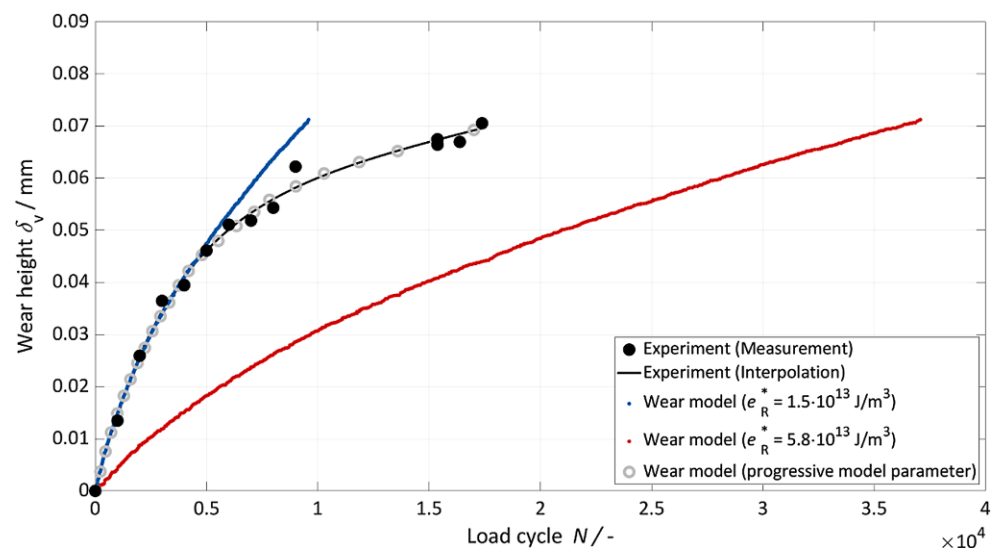
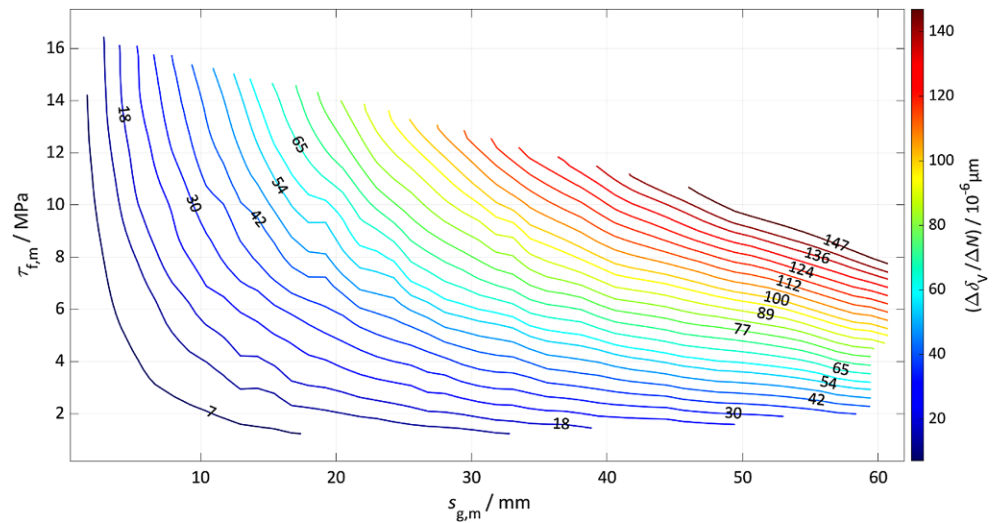




**Fig. 8** Wear rate map with equivalence lines over mean solid frictional shear stress  $\tau_{f,m}$  and mean sliding distance  $s_{g,m}$



was realised with a sectional adaption (four different sections and model parameters) of the modelised wear progression to the experimental data. The result for the wear simulation with progressive model parameter is shown in Fig. 7 with grey markers and approximates the entire experimental wear progression very well. The highest wear energy density of the simulation with a progressive model parameter belongs to a phase close to the steady wear phase. Therefore, this value should be comparable to the results in Sect. 3.3. The mean sliding velocity of the simulated worm gear is  $v_{g,m}=0.15$  m/s. If the diagram from Fig. 2 is considered, the lowest determined wear energy density in this velocity range is equal to  $8.6 \cdot 10^{13}$  J/m<sup>3</sup> and thereby comparable with the value obtained by adapting the wear model to the running-in wear test results.

### 6.3 Simulative study to abrasive wear in worm gears

The purpose of the simulative study was the investigation of abrasive wear for a wide range of worm gear geometries (centre distance  $a=17$ – $250$  mm) and operating conditions with the presented physically-based simulation model. The study was prepared using methods of design of experiment. The focus was on the steady-phase, which is why all analysed worm gear geometries had an ideal contact pattern. Correlations between the calculated wear in this phase and wear-determining parameters were analysed.

As a representative value of the wear progress, a mean wear height was calculated by distributing the accumulated wear volume evenly over the contact area on the worm wheel. The wear rate was obtained by linear regression of the wear progression. From the results of the simulative study, a relationship was determined between the wear rate with respect to the number of load cycles and mean values of the two wear-determining measures solid frictional shear

stress and sliding distance. This correlation is illustrated by the wear map in Fig. 8, which is drawn by interpolating the scattered data points of the simulative study to a regular grid. The wear map indicates equivalence lines for the wear rate with a hyperbolic shape. The hyperbolic shape reflects the proportionality of volumetric wear and solid frictional energy in the energetic wear model (Eq. 2). If Eq. 2 is evaluated locally and divided by the local contact area in a contact point, this proportionality is also given for wear height and the product of solid frictional shear stress and sliding distance. As a conclusion from the simulative results and the wear map, equal wear occurs when the product of the mean solid frictional shear stress  $\tau_{f,m}$  and the mean sliding distance  $s_{g,m}$  is equal. This presumes that the wear energy density is also equal.

For all test points of the study a mean wear energy density  $e_R^*=2.48 \cdot 10^{15}$  J/m<sup>3</sup> from the results in Sect. 3.3 was set, to obtain a wear map for a specific model parameter. However, the used model parameter does not fit to all points of the wear map, since e.g. the size of the gears affects the sliding velocity and, according to Fig. 2, also the model parameter. As wear rate and wear energy density correlate linearly, the wear map can be simply converted to different wear energy densities.

If the mean solid frictional shear stress, mean sliding distance and the wear energy density were known for a worm gearbox, the wear rate could be determined using the wear map. The wear map represents a central element of the practical calculation method for wear in worm gearboxes, developed in the research project related to this work.

## 7 Conclusion and outlook

A wear simulation tool for worm gears was presented, which combines a tribological simulation for tooth friction

with the energetic wear model of Fleischer. The iterative wear modelling procedure allows a transient analysis of local friction and wear by considering the change of the wheel flank geometry. The wear model correlates frictional energy of solid body contacts with volumetric wear removal on the worm wheel using the model parameter wear energy density.

A simulative study was conducted on wear in worm gears operating in the steady-state wear phase. Based on the obtained results, a wear map was presented showing a proportional relationship between mean solid frictional shear stress, mean sliding distance and wear rate in good agreement with the energetic wear model. The wear map allows a simplified calculation of wear in worm gears based on the energetic wear model.

The wear model parameter was determined by combining experimental results of wear tests on worm gearboxes during the steady-state wear phase with calculated results from the tribological simulation. A wide scatter in wear energy density was observed and partially attributed to the differences in sliding velocity. The range of the model parameter is additionally increased by simulative results during the running-in phase, showing a significant influence of the tooth contact situation on the model parameter.

For a reliable calculation of wear, using either the practical method or the complex simulation tool, the wear energy should be reliably determinable without additional worm gear tests. Therefore, an accurate description of the wear energy density is necessary. This requires a thorough analysis of influencing parameters, followed by additional worm gear tests, where these parameters are systematically varied. Consulting studies on wear energy density from literature, this includes the mean flank pressure beside the sliding velocity.

For maximum consistency in the determination of the wear energy density, the experimental data should include both volumetric wear and friction work. However, explicit measurement of tooth friction work in worm gearboxes is difficult due to various sources of power loss. An alternative method is given by twin-disc tribometers, where running conditions as contact pressure and sliding velocity can be precisely adjusted. Tribometer tests also allow direct determination of the friction work in the model contact. A comparison of results from worm gear and tribometer tests can indicate, whether the wear energy density of worm gears could also be determined with tribometer tests, which would significantly reduce the testing effort.

An accurate description is particularly important in the simulation of wear during the running-in phase, where changing tribological conditions also effect the wear energy density. This can be concluded from the validation of the simulation model, where a progressive model parameter leads to the best approximation of the experimental wear

progression during running-in. When the wear progression of the validation test reaches a steady-state wear phase, the wear energy density is in the same order of magnitude as the results from the analysis of the experimental data directly from the steady wear phase. In conclusion, with regard to the global values wear energy density and wear height progression, the wear model gives valid results. A validation of the local wear calculation with local wear measurement on a worm wheel flank will also be an objective for future work.

**Acknowledgements** This work was supported by the German Federal Ministry of Economics and Energy (IGF 19699N) within the framework of the Forschungsvereinigung Antriebstechnik e. V. (FVA project 503 III). The related research project was a collaboration with the Gear Research Centre (FZG) of the Technical University of Munich, which contributed the experimental data to determine the model parameter. For the evaluation of the measured surface data the software *MountainsMap* was used.

**Funding** Open Access funding enabled and organized by Projekt DEAL.

**Conflict of interest** K. Daubach, M. Oehler and B. Sauer declare that they have no competing interests.

**Open Access** This article is licensed under a Creative Commons Attribution 4.0 International License, which permits use, sharing, adaptation, distribution and reproduction in any medium or format, as long as you give appropriate credit to the original author(s) and the source, provide a link to the Creative Commons licence, and indicate if changes were made. The images or other third party material in this article are included in the article's Creative Commons licence, unless indicated otherwise in a credit line to the material. If material is not included in the article's Creative Commons licence and your intended use is not permitted by statutory regulation or exceeds the permitted use, you will need to obtain permission directly from the copyright holder. To view a copy of this licence, visit <http://creativecommons.org/licenses/by/4.0/>.

## References

1. Stachowiak G (2005) *Wear—Materials, Mechanisms and Practice*. John Wiley & Sons, Chichester
2. Fleischer G, Gröger H, Thum H (1980) *Verschleiß und Zuverlässigkeit*. VEB Verlag Technik, Berlin
3. Meng H-C (1994) *Wear modeling: Evaluation and categorization of wear models*. Ph.D.-thesis. University of Michigan,
4. Archard JF (1953) Contact and rubbing of flat surfaces. *J Appl Phys* 24:981–988
5. Jbily D, Guingand M, Vaujany J-P (2016) A wear model for worm gear. *Proceedings of the Institution of Mechanical Engineers—Part C. J Mech Eng Sci* 230(7–8):1290–1302
6. Sharif KJ, Evans HP, Snidle RW (2006) Prediction of the wear pattern in worm gears. *Wear* 261:666–673
7. Pausch S (1998) *Verschleiß von Schneckengetrieben—Theorie und Experiment*. Ph.D thesis. TU, Wien
8. Dauber A (2014) *Analyse, Modellierung und Simulation von Verschleiß auf mehreren Skalen zur Betriebsdauervorhersage von Wellendichtungen aus PTFE-Compound*. Ph.D. thesis. Universität Stuttgart, Stuttgart

9. Boley E (1977) Untersuchung der Parameterabhängigkeit der scheinbaren Reibungsenergiedichte. *Schmieringstechnik* 8(3): 86–88
10. Jennewein B (2016) Integrierter Berechnungsansatz zur Prognose des dynamischen Betriebsverhaltens von Radialwellendichtringen. Ph.D. thesis. Technische Universität, Kaiserslautern
11. Magyar B, Sauer B, Horák P (2012) Tribological investigation of K type worm gear drives. *Acta Polytech Hungarica* 9(6):233–252
12. Predki W (1982) Hertzische Drücke, Schmierpalhöhen und Wirkungsgrade von Schneckengetrieben. Ph.D. thesis., Ruhr-Universität, Bochum
13. Bouché B (1991) Reibungszahlen von Schneckengetrieben im Mischreibungsgebiet. Ph.D. thesis., Ruhr-Universität, Bochum
14. Oehler M, Sauer B, Magyar B (2019) Efficiency of worm gear drives under transient operating conditions. *ASME J Tribol* 141(12): 122201. <https://doi.org/10.1115/1.4044655>
15. Lutz M (2000) Methoden zur rechnerischen Ermittlung und Optimierung von Tragbildern an Schneckengetrieben. Ph.D. thesis. Technische Universität, München
16. Magyar B (2012) Tribo-dynamische Untersuchungen von Zylinderschneckengetrieben. Ph.D.-thesis. Technische Universität, Kaiserslautern
17. Daubach K, Oehler M, Sauer B (2019) A method to determine local wear of worm gears with highly resolved circumferential backlash curves. In: *VDI-Berichte 2355: VDI International Conference on Gears 2019*. VDI Verlag, Düsseldorf, pp 595–606
18. Sappok D (2016) Experimentelle und simulative Methoden zur Untersuchung der Verschleißvorgänge im Kettengelenk von Antriebs- und Steuerketten. Ph.D. thesis. Technische Universität Kaiserslautern, Kaiserslautern